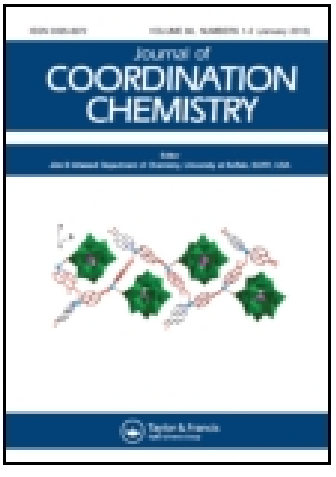

Journal of Coordination Chemistry
Publication details, including instructions for authors and subscription information:
http://www.tandfonline.com/loi/gcoo20

Growth of semiconducting iron sulfide thin films by chemical vapor deposition from air-stable single-source metal organic precursor for photovoltaic application

Sohail Saeed[ab], Rizwan Hussain[b] & Ray J. Butcher[c]

[a] Department of Chemistry, Research Complex, Allama Iqbal Open University, Islamabad, Pakistan

[b] National Engineering & Scientific Commission, Islamabad, Pakistan

[c] Chemistry Department, Howard University, Washington, DC, USA

Accepted author version posted online: 07 May 2014.Published online: 22 May 2014.

To cite this article: Sohail Saeed, Rizwan Hussain & Ray J. Butcher (2014) Growth of semiconducting iron sulfide thin films by chemical vapor deposition from air-stable single-source metal organic precursor for photovoltaic application, Journal of Coordination Chemistry, 67:10, 1693-1701, DOI: 10.1080/00958972.2014.918265

To link to this article: http://dx.doi.org/10.1080/00958972.2014.918265

Journal of Coordination Chemistry, 2014
Vol. 67, No. 10, 1693–1701, http://dx.doi.org/10.1080/00958972.2014.918265

Growth of semiconducting iron sulfide thin films by chemical vapor deposition from air-stable single-source metal organic precursor for photovoltaic application

SOHAIL SAEED*†‡, RIZWAN HUSSAIN‡ and RAY J. BUTCHER§

†Department of Chemistry, Research Complex, Allama Iqbal Open University, Islamabad, Pakistan
‡National Engineering & Scientific Commission, Islamabad, Pakistan
§Chemistry Department, Howard University, Washington, DC, USA

(*Received 27 November 2013; accepted 26 March 2014*)

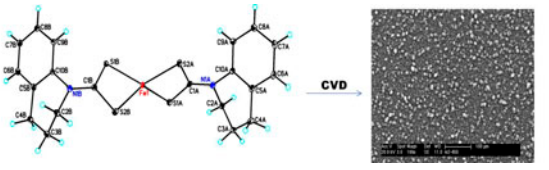

Semiconducting nanostructured iron sulfide thin films were prepared by aerosol chemical vapor deposition at 673 and 723 K from newly synthesized iron complex of dithiocarbo-1,2,3,4-tetrahydroquinoline [$Fe(S_2CNC_9H_{10})_2$]. The degree of film surface roughness was determined by atomic force microscopy. The nature of the deposited thin films formed was determined by a combination of EDX analysis and glancing angle X-ray diffraction.

Keywords: Greigite Fe_3S_4 thin films; Tetrahydroquinoline; p-XRD; Crystallites; SEM; AACVD

Introduction

The application of single-source precursors is becoming a common route for developing nanostructured semiconducting materials. Iron sulfides are an interesting class of materials with different phases, marcasite (calcium chloride structure-FeS_2), mackinawite ($Fe_{1+x}S$), pyrite (cubic-FeS_2), pyrrhotite ($Fe_{1-x}S$, Fe_7S_8), smythite (hexagonal-Fe_3S_4), troilite (FeS), and greigite (cubic spinel-Fe_3S_4) [1, 2]. Iron sulfides exhibit a wide range of properties and applications, from semiconducting, nanomagnetic pyrite (FeS_2) to ferromagnetic Fe_3S_4 [3, 4]. Different types of iron sulfides with various Fe : S ratios, from 0.5 to 1.05, are found in nature. The electrical and magnetic properties of iron sulfides are dependent on the

*Corresponding author. Email: sohail262001@yahoo.com

stoichiometric ratio between iron and sulfur [5, 6]. Among the natural iron sulfide minerals, pyrite and marcasite are diamagnetic; mackinawite is paramagnetic; pyrrhotite and greigite are ferromagnetic; and troilite is antiferromagnetic [7, 8].

Interest has been developed in the synthesis and characterization of iron sulfide thin films [9, 10], due to their potential photovoltaic applications [11]. Whilst the synthesis of iron oxide nanomaterials as insulators is well documented, the deposition of iron chalcogenide [Fe(S, Se, Te)] nanostructured semiconducting thin films and nanomaterials has remained unexplored until recently [12]. O'Brien and co-workers used a series of iron(III) thioburet complexes as single-source precursors for the growth of iron sulfide thin films by aerosol-assisted chemical vapor deposition (AACVD) technique [13].

Herein, we report the use of iron complex of tetrahydroquinoline dithiocarbamate as single-source precursor to prepare semiconducting nanostructured iron sulfide thin films by AACVD.

Experimental

Materials and physical measurements

The synthesis of the iron complex was performed under an inert atmosphere of dry nitrogen using standard Schlenk techniques. Elemental analysis of the complex was performed on a Flash 2000 elemental analyzer. Obtained results were within 0.4% of theoretical values. Metals analysis of the complex was carried out by Thermo iCap 6300 inductively coupled plasma optical emission spectroscopy. Thermogravimetric analysis (TGA) measurement was carried out by a Seiko SSC/S200 model under a heating rate of 283 K min^{-1} under nitrogen. Atmospheric pressure chemical ionization mass spectrometry (MS-APCI) of the iron complex was recorded on a Micromass Platform II instrument. X-ray diffraction (XRD) studies were performed on a Bruker AXSD8 diffractometer using CuKα radiation. SEM analysis was performed using a Philips XL 30FEG.

X-ray structure determination

Single crystal XRD data for the iron complex was collected using graphite-monochromated MoKα radiation ($\lambda = 0.71073$ Å) on an Oxford Diffraction (now Agilent) Gemini-R diffractometer. The structure of the complex was solved by direct methods and refined by full-matrix least-squares [14] based on F^2. All non-hydrogen atoms were refined anisotropically and hydrogens bonded to the carbon atoms were positioned geometrically and allowed to ride on the parent atoms. All calculations were carried out using the SHELXTL package [15].

Synthesis of the iron complex [$Fe(S_2CNTHQ)_2$]

The iron complex was prepared by adopting literature methods [16, 17]. 1,2,3,4-Tetrahydroquinoline (0.01 M) and sodium hydroxide (0.01 M) were mixed in 100 mL of methanol in a beaker with a stirrer. The mixture was cooled to about 273 K in an ice bath while stirring. A solution of carbon disulfide (0.01 M) in ethanol (10 mL) was slowly added to this mixture while vigorously stirring. The mixture was allowed to warm at room temperature after the addition of all carbon disulfides. At this stage, a freshly prepared solution of iron chloride

($FeCl_3 \cdot 6H_2O$) (0.005 M) in ethanol (40 mL) was added drop-wise to the reaction mixture by a dropping funnel. A black precipitate started to form which was filtered after completion of the reaction. The crude product was re-crystallized from chloroform at room temperature to give colorless prism of $[Fe(S_2CNC_9H_{10})_2]$. Yield: 62%, m.p.: decomposition between 519 and 523 K. Elemental analysis: Found: C, 50.75; H, 4.31; N, 5.90; S, 27.14; Fe, 11.80%. Calcd: C, 50.84; H, 4.27; N, 5.93; S, 27.15; Fe, 11.82%. Mass (MS-APCI) (major fragment, *m/z*): 472 [M+, $C_{20}H_{20}FeN_2S_4$].

Growth of iron sulfide thin films by aerosol-assisted chemical vapor deposition

Experiments for deposition of iron sulfide thin films were designed according to the experimental setups (figure 1) of Saeed and co-workers [18–20]. In a typical deposition, 0.25 g of the single-source precursor $[Fe(S_2CNC_9H_{10})_2]$ was dissolved in 15 mL THF in a two-necked 250 mL round-bottom flask with a gas inlet that allowed the carrier gas (argon) to pass into the solution to aid transport of the aerosol. The precursor solution in a round-bottom flask was kept in a water bath above the piezoelectric modulator of a PIFCO ultrasonic humidifier (model no. 1077). The aerosol droplets thus generated were transferred into the hot wall zone of the reactor by carrier gas. The solvent and the precursor were evaporated and the precursor vapor reached the heated glass substrate surface where thermally induced reactions and film deposition took place. Important parameters for the growth of iron sulfide thin films are listed in table 1.

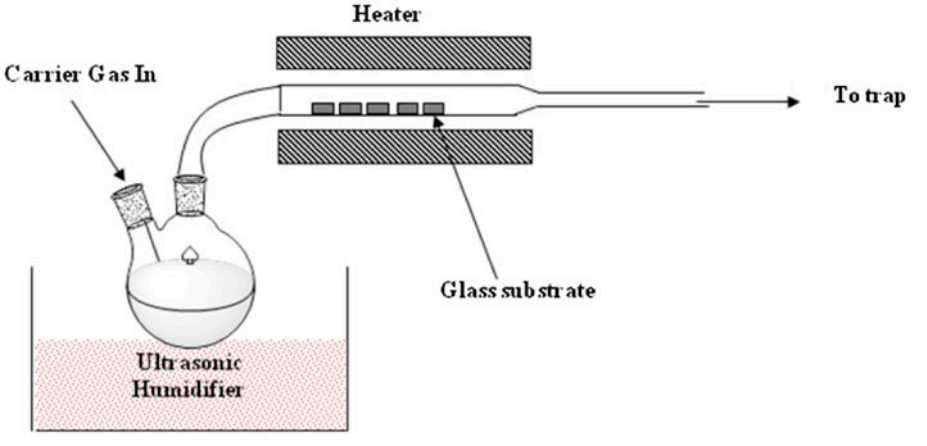

Figure 1. Schematic diagram of an AACVD kit.

Table 1. Growth conditions for the deposition of iron sulfide thin films from precursor.

Iron complex	Precursor conc. (g/15 mL) in THF	Sample injection rate (mL min^{-1})	Carrier gas (argon) flow rate (cm^3 min^{-1})	Reactor temp. (K)	Decomp. time (min)	Deposited phase
$[Fe(S_2CNC_9H_{10})_2]$	0.25	0.17	160	673	90	Fe_3S_4 (greigite)
	0.25	0.17	160	723	90	Fe_3S_4 (greigite)

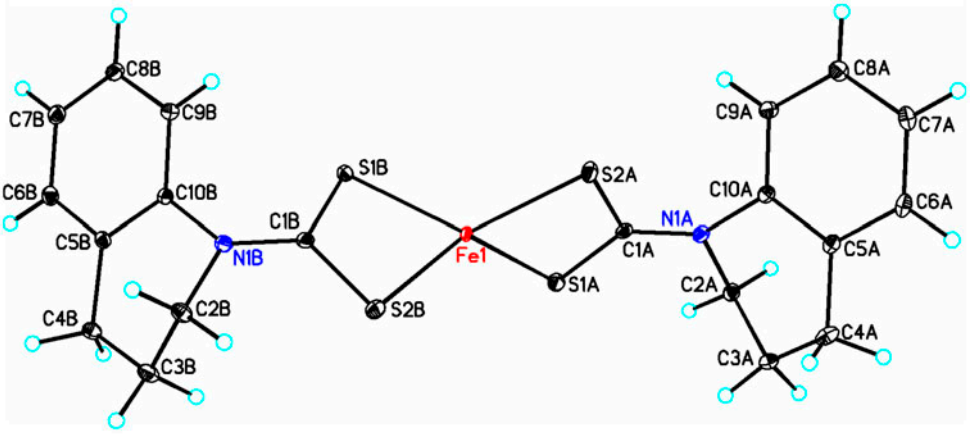

Figure 2. The X-ray single-crystal structure of $[Fe(S_2CNC_9H_{10})_2]$.

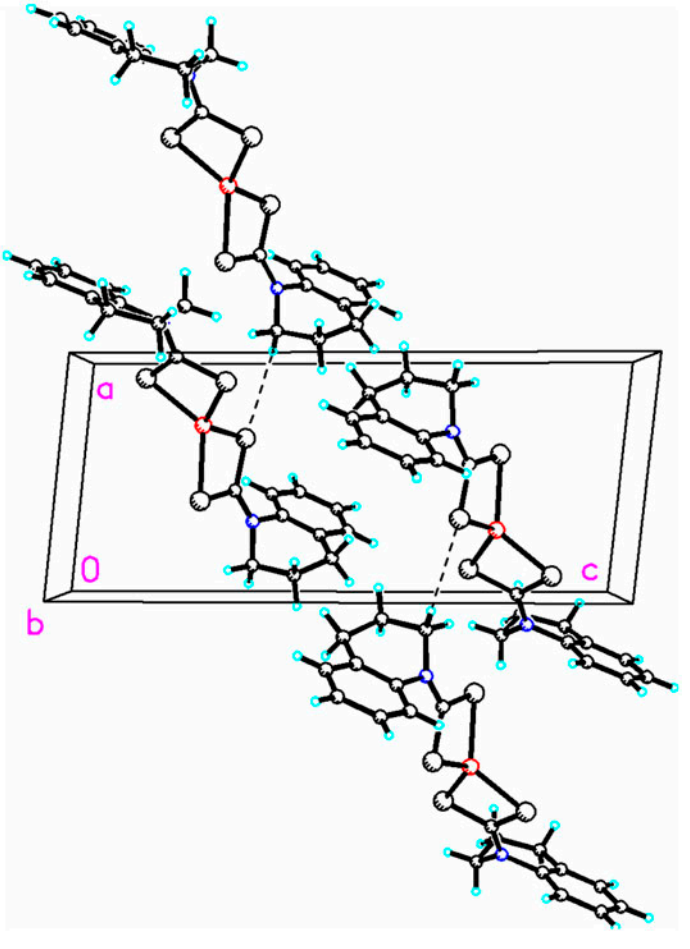

Figure 3. Unit cell diagram of $[Fe(S_2CNC_9H_{10})_2]$.

Results and discussion

Usually, materials reported for construction of photovoltaic cells are either toxic or use less-abundant elements such as lead, cadmium, indium, or gallium. It is desirable to develop less-toxic, easy handling, and cheaper materials even with lower efficiencies. The most promising metal sulfide minerals include iron and copper sulfides.

Single crystal X-ray crystallography

The molecular structure and unit cell diagram of $[Fe(S_2CNC_9H_{10})_2]$ are shown in figures 2 and 3, respectively; crystal data and refinement and selected bond lengths ,and angles are listed in tables 2 and 3, respectively. The X-ray single crystal structure of the iron complex is triclinic with space group *P-1*. The structure is based on a monomeric molecule in which iron is bonded to four sulfurs, two from each tetrahydroquinoline dithiocarbamate. Fe–S bond lengths are 2.303(9)–2.353(9) Å, considerably shorter than those reported for $[Fe(SON(CN^iPr_2)_2)_3]$ (2.418(8) Å) or $[Fe(SON(CNMe_2)_2)_3]$ (2.421(5) Å) [21]. The crystal was a pseudo-merohedral twin with a twin law of {−1 0 0 0 −1 0 −0.49 −0.24 1} and components of 0.672(1) and 0.328(1). The environment about Fe is distorted tetrahedral due to the small bite of the ligands with four-membered chelate rings (bite angles of 78.01(3)° and 78.48(3)°) while the dihedral angle subtended by the two ligands about Fe is close to the expected value of 90° at 86.08(15)°.

Table 2. Crystal data and structure refinement for $[Fe(S_2CNC_9H_{10})_2]$.

CCDC	915366
Empirical formula	$C_{20}H_{20}FeN_2S_4$
Formula weight	472.47
Temperature	123(2) K
Wavelength	0.71073 Å
Crystal system	Triclinic
Space group	*P-1*
Unit cell dimensions	$a = 7.5062(5)$ Å $\alpha = 86.733(7)°$ $b = 7.5863(7)$ Å $\beta = 83.805(6)°$ $c = 17.5907(15)$ Å $\gamma = 87.357(6)°$
Volume	993.42(14) Å^3
Z	2
Density (calculated)	1.580 Mg m^{-3}
Absorption coefficient	1.188 mm^{-1}
F (0 0 0)	488
Crystal size	0.55 × 0.31 × 0.27 mm^3
Theta range for data collection	3.08°–37.70°
Index ranges	$-12 \le h \le 12$, $-12 \le k \le 12$, $-30 \le l \le 29$
Reflections collected	12383
Independent reflections	12383 [R(int) = 0.0000]
Completeness to theta = 25.50°	99.8%
Absorption correction	Semi-empirical from equivalents
Max. and min. transmission	1.00000 and 0.89825
Refinement method	Full-matrix least-squares on F^2
Data/restraints/parameters	12383/0/245
Goodness-of-fit on F^2	1.029
Final R indices [$I > 2\sigma(I)$]	$R_1 = 0.0705$, $wR_2 = 0.1945$
R indices (all data)	$R_1 = 0.0952$, $wR_2 = 0.2080$
Largest diff. peak and hole	2.110 and −1.326 e Å^{-3}

Thermogravimetric analysis

Thermogram of $[Fe(S_2CNC_9H_{10})_2]$ shows two stages of weight loss (figure 4). The first step begins at 451 K and ends at 593 K. The second one starts at 597 K and is completed at 858 K, with the residue amounting to 20.74% at 858 K of the initial weight. The residual weight (20.74%) is close to the expected composition for FeS (calcd 17.79%), the presence of which was further supported by XRD analysis of the residue.

Crystalline phases and stoichiometry identification by XRD studies

In order to identify the crystalline phases of iron sulfide in the deposited semiconducting nanostructured thin films, XRD analysis was performed. Using the above TGA data, the AACVD experiments were run at 623, 673, and 723 K. The iron complex $[Fe(S_2CNC_9H_{10})_2]$ gave no product at a growth temperature of 623 K (figure 5) but at growth temperatures of 673 and 723 K, gave almost pure greigite (Fe_3S_4) phase. The diffraction peaks for (111), (220), (311), (400), (511), and (440) planes of greigite (Fe_3S_4) were dominant (ICDD NO: 00-016-0713). The iron complex does not produce any product at 623 K and gives a pure greigite (Fe_3S_4) at 673 and 723 K.

Table 3. Bond lengths [Å], bond angles [°], and torsion angles [°] for $[Fe(S_2CNC_9H_{10})_2]$.

Bond lengths	
Fe(1)–S(1B)	2.3035(9)
Fe(1)–S(2A)	2.3347(10)
Fe(1)–S(1A)	2.3538(9)
S(1A)–C(1A)	1.723(3)
S(2A)–C(1A)	1.723(3)
S(2B)–C(1B)	1.736(3)
N(1A)–C(1A)	1.332(4)
N(1A)–C(2A)	1.474(4)
Bond angles	
S(1B)–Fe(1)–S(2A)	128.57(4)
S(1B)–Fe(1)–S(1A)	127.34(4)
S(2A)–Fe(1)–S(1A)	78.01(3)
S(2A)–Fe(1)–S(2B)	123.23(4)
S(1A)–Fe(1)–S(2B)	128.86(4)
N(1A)–C(1A)–S(2A)	121.2(3)
N(1A)–C(1A)–S(1A)	120.9(2)
S(2A)–C(1A)–S(1A)	117.84(19)
N(1B)–C(1B)–S(1B)	122.2(3)
Torsion angles	
S(1B)–Fe(1)–S(2A)–C(1A)	−131.76(11)
S(1A)–Fe(1)–S(2A)–C(1A)	−3.18(11)
S(2B)–Fe(1)–S(2A)–C(1A)	125.69(11)
S(2A)–Fe(1)–S(1B)–C(1B)	−122.66(12)
S(1A)–Fe(1)–S(1B)–C(1B)	131.43(11)
S(1B)–Fe(1)–S(2B)–C(1B)	−0.90(11)
S(2A)–Fe(1)–S(2B)–C(1B)	127.95(11)
S(1A)–Fe(1)–S(2B)–C(1B)	−130.00(11)

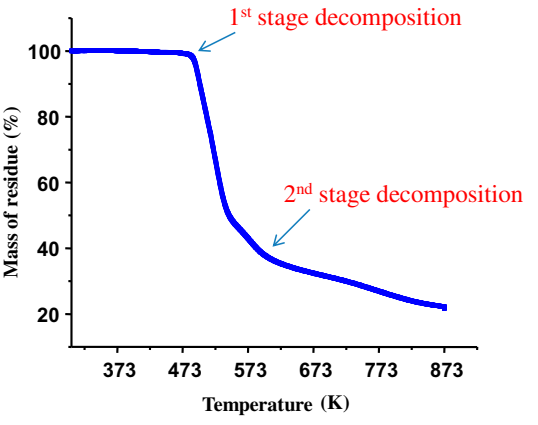

Figure 4. TGA of $[Fe(S_2CNC_9H_{10})_2]$ at heating rate of 283 K min^{-1} under nitrogen; flow rate of nitrogen was 100 mL min^{-1}.

Scanning electron and atomic force microscopic studies

SEM images of iron sulfide thin films (figure 6) deposited at 673 and 723 K show small flower-like clusters with an average size of 5–10 µm. EDX analysis shows that the iron sulfide thin films have iron: sulfur ratio 41 : 59 (673 and 723 K).

Atomic Force Microscopy (AFM) is an imaging technique that is widely used due to its high resolution and large array of materials it can analyze (dielectrics, conductors, biological materials, etc.). It provides a 3-D profile of the surface on a nanoscale, by measuring forces between a sharp probe (<10 nm) and surface at very short distance (0.2–10 nm probe-sample separation). Its applications include examining semiconductor wafers or

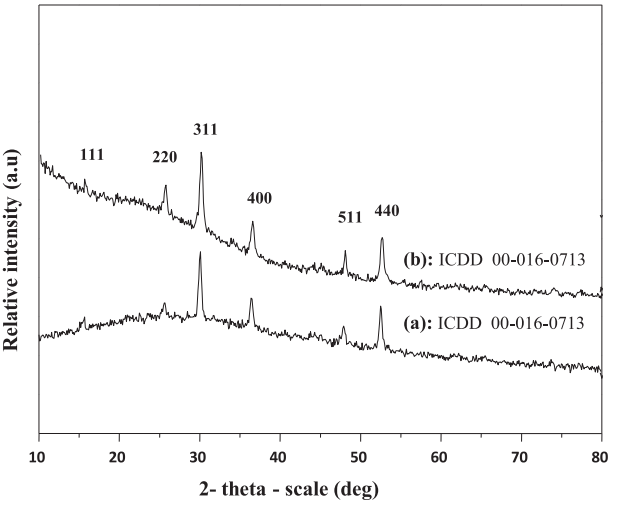

Figure 5. p-XRD pattern of the iron sulfide thin film deposited from iron complex $[Fe(S_2CNC_9H_{10})_2]$ at (a) 673 and (b) 723 K.

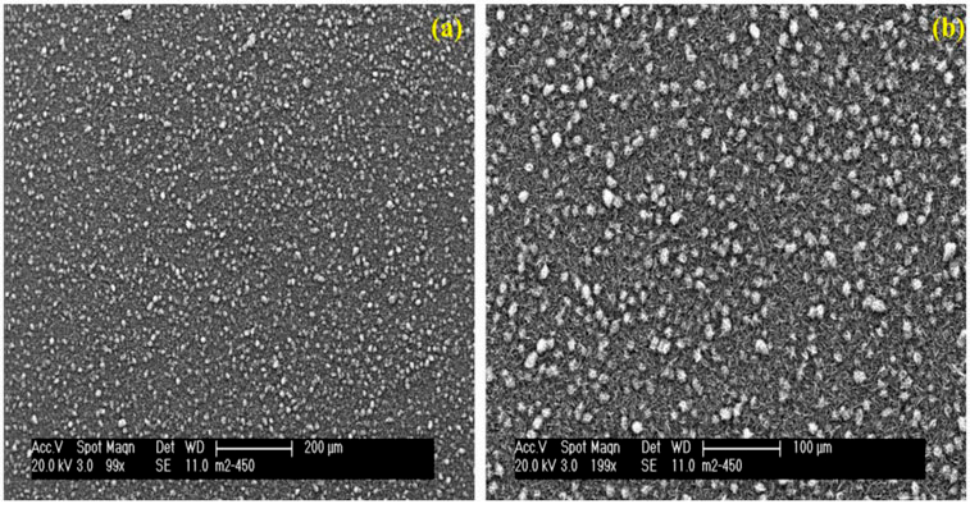

Figure 6. SEM images of iron sulfide thin films deposited from iron complex $[Fe(S_2CNC_9H_{10})_2]$ at (a) 673 and (b) 723 K.

evaluating the impact of surface roughness on the adhesion properties of a material. This sophisticated and advanced technique is among the best tools for surface characterization of semiconducting materials. Its 2-D and 3-D images provide accurate quantitative information of thin film roughness. The 3-D AFM image of the film (figure 7) shows the growth of closely packed crystallites onto a glass substrate at 723 K with an average roughness of 10.75 nm and rms roughness 15.12 nm.

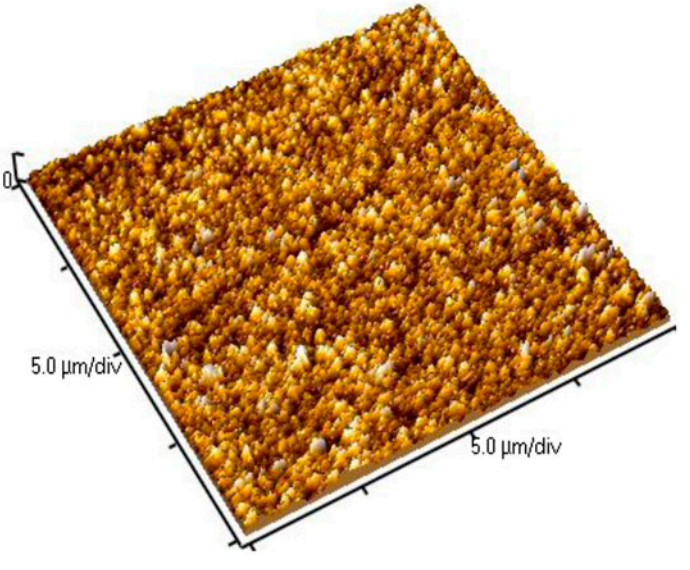

Figure 7. AFM image in 3-D view of iron sulfide thin film deposited at 723 K.

Conclusion

The iron complex of tetrahydroquinoline dithiocarbamate $[Fe(S_2CNC_9H_{10})_2]$ has been synthesized and its structure was determined by X-ray single crystallography. AACVD of the deposited iron sulfide (Fe_3S_4) thin films at 673 and 723 K has small flower-like crystallites. AFM studies showed that the average roughness and rms roughness of deposited semiconducting nanostructured iron sulfide thin film were 10.75 and 15.12 nm, respectively.

Supplementary material

Crystallographic data for the structure reported in this article have been deposited with Cambridge Crystallographic Data Center, CCDC 915366. Copies of this information may be obtained free of charge from the Director, CCDC, 12 Union Road, Cambridge, CBZ IEZ, UK. Facsimile: (44) 01223 336 033, E-mail: deposit@ccdc.cam.ac.uk or http://www.ccdc.cam.ac.uk/deposit.

Acknowledgment

Dr Sohail Saeed would like to acknowledge the Higher Education Commission (HEC), Government of Pakistan for financial support. RJB wishes to acknowledge the NSF-MRI program (Grant CHE-0619278) for funds to purchase the diffractometer.

References

[1] M. Akhtar, J. Akhter, M.A. Malik, P. O'Brien, F. Tuna, J. Raftery, M. Helliwell. *J. Mater. Chem.*, **21**, 9737 (2001).
[2] C.N.R. Rao, K.P.R. Pisharody. *Prog. Solid State Chem.*, **10**, 207 (1976).
[3] H. Wang, I. Salveson. *Phase Trans.*, **78**, 547 (2005).
[4] C.I. Pearce, R.A.D. Pattrick, D.J. Vaughan. *Rev. Mineral. Geochem.*, **61**, 127 (2006).
[5] J.C. Ward. *Rev. Pure Appl. Chem.*, **20**, 175 (1970).
[6] D. Rickard, G.W. Luther. *Chem. Rev.*, **107**, 514 (2007).
[7] E. Makovicky. *Rev. Mineral. Geochem.*, **61**, 7 (2006).
[8] D.J. Vaughan, J.R. Craig. *Mineral Chemistry of Metal Sulfides*, Cambridge University Press, Cambridge (1978).
[9] S. Seefeld, M. Limpinsel, Y. Liu, N. Farhi, A. Weber, Y. Zhang, N. Berry, Y.J. Kwon, C.L. Perkins, J.C. Hemminger, R. Wu, M. Law. *J. Am. Chem. Soc.*, **135**, 4412 (2013).
[10] A.N. Gleizes. *Chem. Vap. Deposition*, **6**, 155 (2000).
[11] S. Kar, S. Chaudhuri. *Mater. Lett.*, **59**, 289 (2005).
[12] Y. Zhang, Y. Du, H. Xu, Q. Wang. *CrystEngComm*, **12**, 3658 (2010).
[13] K. Ramasamy, M.A. Malik, M. Helliwell, F. Tuna, P. O'Brien. *Inorg. Chem.*, **49**, 8495 (2010).
[14] G.M. Sheldrick. *SHELXS-97 and SHELXL-97*, University of Gottingen, Germany (1997).
[15] Bruker. *SHELXTL (Version 6.12)*, Bruker AXS Inc., Madison, WI (2001).
[16] M.A. Malik, N. Revaprasadu, P. O'Brien. *Chem. Mater.*, **13**, 913 (2001).
[17] P.S. Nair, T.R.N. Radhakrishnan, G.A. Kolawole. *J. Mater. Chem.*, **11**, 1555 (2001).
[18] S. Saeed, N. Rashid, M.A. Malik, P. O'Brien, W.-T. Wong. *New J. Chem.*, **37**, 3214 (2013).
[19] S. Saeed, N. Rashid, K.S. Ahmad. *Turk J. Chem.*, **37**, 796 (2013).
[20] S. Saeed, N. Rashid, M.A. Malik, P. O'Brien, W.-T. Wong. *J. Coord. Chem.*, **66**, 2788 (2013).
[21] P.J. Thomas. *Annu. Rep. Prog. Chem., Sect. A: Inorg. Chem.*, **109**, 453 (2013).